AFRL-RX-WP-JA-2015-0036

CHARACTERIZATION OF CREASES IN POLYMERS FOR ADAPTIVE ORIGAMI STRUCTURES (POSTPRINT)

Philip R. Buskohl
UES, Inc.

Richard A. Vaia
AFRL/RXA

James J. Joo and Gregory W. Reich
AFRL/RQV

Andrew C. Abbott
University of Dayton

OCTOBER 2014
Interim Report

Distribution A. Approved for public release; distribution unlimited.

See additional restrictions described on inside pages

STINFO COPY

AIR FORCE RESEARCH LABORATORY
MATERIALS AND MANUFACTURING DIRECTORATE
WRIGHT-PATTERSON AIR FORCE BASE, OH 45433-7750
AIR FORCE MATERIEL COMMAND
UNITED STATES AIR FORCE

NOTICE AND SIGNATURE PAGE

Using Government drawings, specifications, or other data included in this document for any purpose other than Government procurement does not in any way obligate the U.S. Government. The fact that the Government formulated or supplied the drawings, specifications, or other data does not license the holder or any other person or corporation; or convey any rights or permission to manufacture, use, or sell any patented invention that may relate to them.

This report was cleared for public release by the USAF 88th Air Base Wing (88 ABW) Public Affairs Office (PAO) and is available to the general public, including foreign nationals.

Copies may be obtained from the Defense Technical Information Center (DTIC) (http://www.dtic.mil).

AFRL-RX-WP-JA-2015-0036 HAS BEEN REVIEWED AND IS APPROVED FOR PUBLICATION IN ACCORDANCE WITH ASSIGNED DISTRIBUTION STATEMENT.

//Signature//

RICHARD A. VAIA
Functional Materials Division
Materials and Manufacturing Directorate

//Signature//

KAREN R. OLSON, Deputy Chief
Functional Materials Division
Materials and Manufacturing Directorate

//Signature//

TIMOTHY J. BUNNING, Chief
Functional Materials Division
Materials and Manufacturing Directorate

This report is published in the interest of scientific and technical information exchange, and its publication does not constitute the Government's approval or disapproval of its ideas or findings.

REPORT DOCUMENTATION PAGE

Form Approved
OMB No. 074-0188

1. REPORT DATE (DD-MM-YYYY)	2. REPORT TYPE	3. DATES COVERED *(From – To)*
October 2014	Interim	08 June 2011 – 08 September 2014

4. TITLE AND SUBTITLE
CHARACTERIZATION OF CREASES IN POLYMERS FOR ADAPTIVE ORIGAMI STRUCTURES (POSTPRINT)

5a. CONTRACT NUMBER
In-House

5b. GRANT NUMBER

5c. PROGRAM ELEMENT NUMBER
61102F

6. AUTHOR(S)
(see back)

5d. PROJECT NUMBER
3001

5e. TASK NUMBER

5f. WORK UNIT NUMBER
X091

7. PERFORMING ORGANIZATION NAME(S) AND ADDRESS(ES)
(see back)

8. PERFORMING ORGANIZATION REPORT NUMBER

9. SPONSORING / MONITORING AGENCY NAME(S) AND ADDRESS(ES)
Air Force Research Laboratory
Materials and Manufacturing Directorate
Wright Patterson Air Force Base, OH 45433-7750
Air Force Materiel Command
United States Air Force

10. SPONSOR/MONITOR'S ACRONYM(S)
AFRL/RXA

11. SPONSOR/MONITOR'S REPORT NUMBER(S)
AFRL-RX-WP-JA-2015-0036

12. DISTRIBUTION / AVAILABILITY STATEMENT
Distribution A. Approved for public release; distribution unlimited. This report contains color.

13. SUPPLEMENTARY NOTES
PA Case Number: 88ABW-2014-2964, Clearance Date: 16 June 2014. Journal article published in ASME 2014 Smart Materials, Adaptive Structures and Intelligent Systems. The final publication is available at doi:10.1115/SMASIS2014-7480.

14. ABSTRACT
Techniques employed in origami are of interest for the design of actuating structures with multiple defined geometric states. Most research in this area has focused on manipulating material chemistry or geometry to achieve folding, but crease development through full material thickness has not been studied in detail. Understanding creasing is crucial for establishing material selection guidelines in origami engineering applications. Identification of the precise failure mechanisms is critical for understanding the residual fold angle and selecting optimal materials for specific origami applications. To characterize crease formation and development, polymer films were folded using a modified parallel plate bending technique which was successfully modeled with Euler beam theory in the elastic regime. Fold angles measured after creasing provided a means to quantitatively describe a material's ability to retain a fold, and degree of plastic deformation incurred during folding. SEM micrographs of creased regions revealed tensile deformations on exterior crease surfaces while compressive deformations such as wrinkling occurred inside. Profilometry was performed on crease interiors to identify and measure wrinkle topology. It was found that increased dissipative plastic deformation led to retention of smaller fold angles. These characterization techniques can be used as a means of classifying and organizing polymers by potential usefulness in structural origami applications.

15. SUBJECT TERMS
force, moment of inertia, bending moment, radius of curvature, glycol-modified poly, polypropylene, width, moment arm, thickness, stress, strain, fold angle

16. SECURITY CLASSIFICATION OF:			17. LIMITATION OF ABSTRACT	18. NUMBER OF PAGES	19a. NAME OF RESPONSIBLE PERSON *(Monitor)*
a. REPORT	b. ABSTRACT	c. THIS PAGE			Richard A. Vaia
Unclassified	Unclassified	Unclassified	SAR	11	19b. TELEPHONE NUBER *(include area code)* (937) 255-9209

REPORT DOCUMENTATION PAGE Cont'd

6. AUTHOR(S)

Philip R. Buskohl - UES, Inc.
Richard A. Vaia- Materials and Manufacturing Directorate, Air Force Research Laboratory, Functional Materials Division
James J. Joo and Gregory W. Reich - Air Force Research Laboratory, Aerospace Systems Directorate
Andrew C. Abbott - University of Dayton

7. PERFORMING ORGANIZATION NAME(S) AND ADDRESS(ES)

UES Inc.
4401 Dayton-Xenia Rd.
Dayton, OH 45432

AFRL/RXA
Air Force Research Laboratory
Materials and Manufacturing Directorate
Wright-Patterson Air Force Base, OH 45433-7750

AFRL/RQV
Air Force Research Laboratory
Aerospace Systems Directorate
Wright-Patterson Air Force Base, Ohio 45433

University of Dayton
300 College Park
Dayton, Ohio 45469

Proceedings of the ASME 2014 Conference on Smart Materials, Adaptive Structures and Intelligent Systems
SMASIS2014
September 8-10, 2014, Newport, Rhode Island, USA

SMASIS2014-7480

CHARACTERIZATION OF CREASES IN POLYMERS FOR ADAPTIVE ORIGAMI STRUCTURES

Andrew C. Abbott[1,2,4], Philip R. Buskohl[1,2], James J. Joo[3], Gregory W. Reich[3], Richard A. Vaia[2]

[1]UES Inc,.
4401 Dayton-Xenia Rd.
Dayton, OH 45432

[2]Air Force Research Laboratory, Materials and Manufacturing Directorate
Wright-Patterson AFB, Ohio, USA

[3]Air Force Research Laboratory, Aerospace Systems Directorate
Wright-Patterson AFB, Ohio, USA

[4]University of Dayton
300 College Park
Dayton, Ohio, USA

ABSTRACT

Techniques employed in origami are of interest for the design of actuating structures with multiple defined geometric states. Most research in this area has focused on manipulating material chemistry or geometry to achieve folding, but crease development through full material thickness has not been studied in detail. Understanding creasing is crucial for establishing material selection guidelines in origami engineering applications. Identification of the precise failure mechanisms is critical for understanding the residual fold angle and selecting optimal materials for specific origami applications. To characterize crease formation and development, polymer films were folded using a modified parallel plate bending technique which was successfully modeled with Euler beam theory in the elastic regime. Fold angles measured after creasing provided a means to quantitatively describe a material's ability to retain a fold, and degree of plastic deformation incurred during folding. SEM micrographs of creased regions revealed tensile deformations on exterior crease surfaces while compressive deformations such as wrinkling occurred inside. Profilometry was performed on crease interiors to identify and measure wrinkle topology. It was found that increased dissipative plastic deformation led to retention of smaller fold angles. These characterization techniques can be used as a means of classifying and organizing polymers by potential usefulness in structural origami applications.

NOMENCLATURE

F	Force
I	Moment of inertia
M	Bending moment
R	Radius of curvature
PETG	Glycol-modified poly(ethylene terephthalate)
PP	Polypropylene
b	Width
d	Moment arm
t	Thickness
σ	Stress
ε	Strain
θ	Fold angle

INTRODUCTION

The function of a device is inherently dependent on its shape. By extension, a device that can change shape may possess multiple functions. Examples of shape change to drive function include deployable solar arrays [1] and antennas [2]. Solar array ratio of deployed to compact diameter is minimized to enable efficient packaging for launch and large surface area

for maximum energy collection in space. Shape change is seen in origami when a flat sheet of paper is folded into a complex geometry or model. Origami is not limited to artistic design; it holds great potential as a design tool for engineers striving to obtain shape change to alter device performance. Origami principles have recently been studied to facilitate design of efficient shape change through folding motions [3-5]. Of particular interest are origami patterns capable of actuation, the ability to transition between two or more states upon application of some external load. An avenue to achieve this type of shape change that has recently received significant attention is activation of stimuli-responsive materials [6-8]. A stiff substrate material such as paper or polymer film may be used to support active materials to achieve desired structural integrity. In other cases, origami principles can be applied to design structures which can absorb a greater amount of energy upon impact [9,10]. Generally, one must understand folding behavior in any material selected for an origami application.

Important to material selection in any engineering design is the ability to evaluate a variety of materials by standardized metrics to determine which is best for a particular application. Unfortunately, fold performance is currently not well defined across different material types. For paper, traditionally used in origami art and packaging, excellent correspondence between material properties and performance is known. For example, studies examining paperboard for packaging industries developed creasing and folding setups and described, in great detail, corresponding material behavior [11-13]. Creasing is achieved by indentation of paperboard to generate uniform folding lines by localizing stress and altering geometry [14]. Folding is then carried out by two, three, or four-point bending or by another in-house method in the opposite direction of creasing. Paperboard compressive strength is a key factor in determining onset of failure in the form of delamination [15]. Failure mechanisms of paper (delamination and buckling) however are fundamentally different than those of polymer films. Unfortunately, these established experimental procedures are limited by either attainable maximum bending strain or fold angle and are not sufficient to capture failure in polymers.

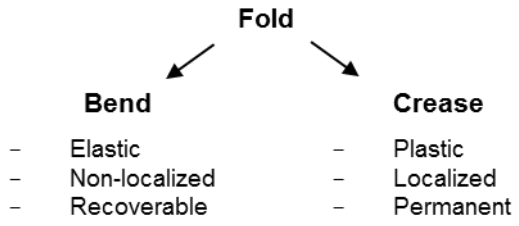

Relevant fold performance metrics will thus depend on the intended use, as well as the mechanical behavior and failure mechanism of the material. To this end, a more precise engineering definition of fold, bend, and crease, is required to characterizing fold performance across material types. For the purposes of this study the following definitions apply to the noun forms of these terms. A fold is any curvature of a plate resulting in a deviation from a flat state. This can be accompanied by either elastic or plastic deformation necessitating two sub categorical definitions. “Bend” is the term associated with elastic, recoverable, non-local curvature and is characterized by complete restorative force-deformation behavior. A constant applied force is required to maintain a bend. The term “crease” is assigned to folds involving permanent, non-recoverable, and localized plastic deformation. Ideally, a crease will have complete dissipative force-deformation behavior, but some restorative behavior is typically present, especially in polymers. Fold performance is thus a broad term that describes material response to folding.

Numerous engineering metrics can be envisioned to quantify the impact of a material on fold performance, including energy dissipation on increasing number of folding events about existing fold lines, residual fold angle or fold hold, and angle opening or relaxation over time. As an example, an origami artist working with our research group defined four categories based on his desired characteristics. The categories were: crease memory, reversibility, accuracy, and hold. Memory refers to the ability of a material to retain crease lines and re-fold about them. For example, a perfectly elastic material would have no crease memory. Reversibility involves folding in the opposite direction about an existing crease. Paper can easily be folded back around an existing crease line and thus is highly reversible; however a material with low reversibility would incur a new crease. Accuracy describes the ability to form a straight fold line connecting two points, a feat that may be difficult for a strongly anisotropic material or one with large morphological features. Hold was designated as residual fold angle with complete hold marked by no residual angle (aluminum foil) and zero hold by full unfolding (PDMS). These fold performance categories reflect the artist’s primary goal to create precise folds to construct an aesthetically pleasing model. Engineering applications on the other hand may be more concerned with other factors, such as the amount of energy needed to fold, fatigue behavior, relaxation time, recoil force, etc.

While developing approaches to quantify all these metrics is important, the work presented here focuses on characterizing folding of polymers by fold angle retention and amount of plastic deformation. This metric serves as an initial parameter for eliminating possible adaptive materials for design of active origami structures. Qualitatively, the relative ability of a film to maintain a fold can be easily compared with a simple empirical ranking on a scale of 1-5. Although adequate for artists with extensive experience, broad engineering material selection requires protocol that factors both geometric and material effects for direct comparison between options. The approach taken herein consists of a few steps. First, fold performance criteria were identified and defined as a way to qualitatively understand and compare folding between materials and geometries. Second, methods were developed to fold materials and describe them quantitatively. To accomplish this, a folding

technique was utilized to fold select polymers to closure. Fold angle relaxation was measured over time serving as a means of comparing fold performance of different materials. Third, failure modes occurring locally in response to fold formation were examined to further understand material-specific influence on fold performance.

MATERIALS & METHODS

Kapton, polypropylene (PP), and glycol-modified poly(ethylene terephthalate) (PETG) were chosen for this study such that a range of polymer properties were covered. Kapton HN films from The DuPont Company in thicknesses of 27, 52, 76, and 127 μm were studied. Kapton is a high performance polyimide thermoplastic characterized by high Tg and stiffness. Polypropylene acquired from DOW Chemical (42 μm thick) and Grafix (510 μm thick) is a commodity thermoplastic capable of strain-induced crystallization which accounts for its high fatigue life. PETG from Transilwrap (127 μm thick) is an amorphous film characterized by moderate stiffness and some degree of stress-whitening in response to applied stresses.

Commercial origami paper (62 μm thick) was acquired from an arts and crafts retailer and served as comparison between a more traditional origami material and polymers. Additionally, Hewlett-Packard printer paper (105 μm thick) served as another baseline material. Both papers had distinct, observable directionality caused by preferential fiber alignment.

A technique was developed to form folds in polymer and paper specimens using a TA Instruments RSA3 in parallel plate compression mode (Fig. 1(a)). Specimens with dimensions of 25 mm (1 in) length and 13 mm (0.5 in) width were bent to fit between 25 mm (1 in) diameter plates spaced at 10 mm. They were fixed to the bottom plate with tape to remain stationary and free on the top plate to allow sliding to relieve compressive stresses at the tape (Fig. 1(b)). Other boundary conditions were explored including taping to both plates, adhering sandpaper to the top plate, and free on both plates. Taping to both plates often caused bending in multiple locations on the specimen due to any misalignment. Sandpaper suffered from similar issues. Free conditions allowed slipping and occasionally specimens completely slipped out between the plates. Compression was performed with a rate of 10 mm/min to a radius of curvature-thickness ratio (R/t) of unity. In all cases, folds were formed perpendicular to the machine direction so that the maximum folding force with respect to material orientation was measured. Force and displacement were recorded for both loading and unloading cycles from which stress/strain data were calculated using Euler elastic beam theory. This theory is limited to elastic deformation and was applied only outer surfaces subjected to maximum bending strain. Calculations were only performed for the outer surfaces where the stresses were at a maximum so that a comparison between bending and stretching could be made. Equation (1) gives the relations used to calculate bending stress and strain where M is the bending moment, F is the applied force, d is the length of the moment arm or the perpendicular distance between the direction and location of applied load and the fold vertex, t is the material thickness, I is the moment of inertia equal to $(bt^3)/12$ where b is the specimen width, and R is the radius of curvature.

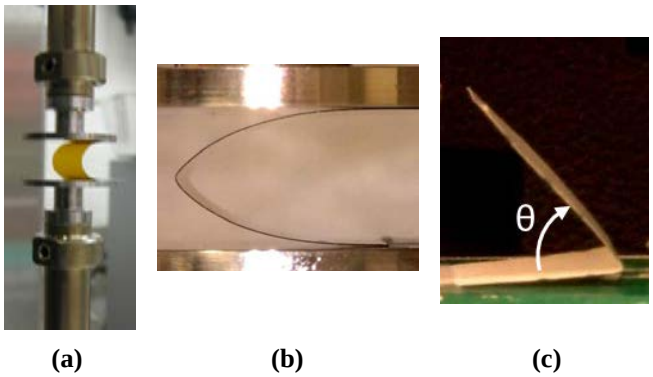

(a) (b) (c)

FIGURE 1: (a) PARALLEL PLATE FOLDING SETUP (b) FOLDED SPECIMEN, SIDE VIEW (c) RELAXATION ANGLE

$$M = Fd, \quad \sigma = Mt/(2I), \quad \varepsilon = t/(2R) \qquad (1)$$

Tensile tests were performed to confirm bending stress/strain results and also to check if common tensile properties could serve as indicators of fold performance. A Tinius Olsen H10KS bench top mechanical tester was used with tensile grips powered by compressed nitrogen gas with a gripping pressure of 40 psi. Specimens were prepared to dimensions of 4 mm width and 25 mm (1in) gauge length. A crosshead speed of 10 mm/min was applied until specimen failure occurred.

After creating folds with the parallel plate technique, fold angle relaxation was tracked as the interior opening angle after removal of applied load (Fig. 1(c)). Thickness effects on fold angle relaxation were first compared using four thicknesses of Kapton. Experiments were then extended to origami paper and polymers which were compared for a time period of 6 hours, after which equilibrium was reached. This served as a way to compare folding for a variety of materials.

A Bruker contact profilometer with a 2 μm radius stylus with a contact force of 3 mg was used to measure height profiles of permanent deformation in fold interiors. Data was recorded with a range of 65.5 μm with 85% of the range reserved for depths less than the initial starting position height. This ensured capture of features inside the valley-shaped residual curvature of the folded region caused by permanent deformation. Curvature was accounted for by fitting the data with a quadratic equation to smooth the curve.

Plastic deformation associated with polymer yielding was examined with an FEI Quanta scanning electron microscopy (SEM). Specimens were sputter coated with Au-Pd alloy for 60 seconds to form a conductive layer on the surface. Beam voltage was set to 5 kV with a spot size of 3 and an aperture of 30 μm. Only the secondary electron detector was used to capture micrographs.

TABLE 1: UNIAXIAL TENSILE PROPERTIES

Material	Young's Modulus (GPa)	Yield Strain (%)
Kapton	2.48 ± 0.2	3.36 ± 0.9
PETG	1.49 ± 0.1	4.73 ± 0.3
PP	0.99 ± 0.1	4.44 ± 0.4
Printer Paper	2.76 ± 0.4	1.01 ± 0.3
Origami Paper	4.07 ± 0.1	0.98 ± 0.3

RESULTS AND DISCUSSION

Tensile experiments yielded Young's modulus, yield strain, and strain at break which were compared between polymer films and origami paper as seen in Table 1. Comparing these to empirical assessments of crease memory, reversibility, accuracy, and hold, possible correlations were explored to establish a key factor underlying performance, such as compressive strength known for paper and cardboard. Unfortunately, no strict correlations could be found. Polymers tended to have lower stiffness and higher yield strain than paper, but some polymers held a fold quite well compared to paper while others did not.

Parallel plate folding was used to generate folds in polymer films and origami paper. Equation (1) was used to calculate bending stress/strain based on force displacement data collected from the parallel plate folding technique. Good agreement was found between bending and tensile results in the elastic regime (Fig. 2) thus validating the experimental procedure. The comparison breaks down after the onset of plastic deformation by as much as 50% due to the assumptions of parallel planes remain plane and a linear constitutive theory in Euler bending. Insets in Fig. 2 show stress fields for applied tension and bending where the dashed line represents the neutral axis in bending.

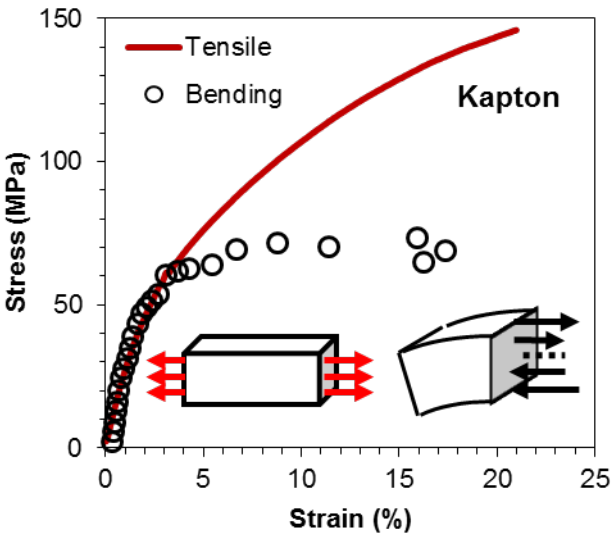

FIGURE 2: COMPARISON OF BENDING TO TENSILE STRESS/STRAIN

TABLE 2: FOLD ANGLE RELAXATION RESULTS

Material	Thickness (μm) ±2	Initial Angle (t = 0) ± 3°	Final Angle (t = 6 hr) ± 3°	Angle Increase
Kapton	25	133	150	17
Kapton	52	114	137	23
Kapton	76	103	133	30
Kapton	127	99	122	23
PP	42	104	128	24
PETG	127	2	<5	3
Printer Paper	105	48	79	31
Origami Paper	62	28	54	26

Thickness presents a tunable geometrical factor incorporated into the angle retention metric and its effects on equilibrium fold angle were first examined with four thicknesses of Kapton film measuring 25, 52, 76, and 127 μm (1, 2, 3, 5 mil). Fold angles were measured as shown in Fig. 1(c). Tracking fold angle over six hours revealed that equilibrium fold angle decreased with increasing thickness as reported in Table 2. This was attributed to larger surface strains induced on thicker films when all films were folded to the same R/t. One might expect that increasing thickness should also increase fold angle. This would be true if all specimens were loaded with equal force. However, all specimens were loaded to the same radius to thickness ratio and therefore larger forces were applied to thicker specimens. This induced more plastic deformation which ultimately has the greatest impact on residual fold angle.

Measurements of equilibrium fold angles were extended to PP, PETG, printer paper, and origami paper to examine material effects on the angle retention metric. Because not all film thicknesses were equal, these materials could only be directly compared to Kapton. It was found that equilibrium angle was not only affected by thickness, but also had a distinct material dependence. For example, Table 2 shows PETG retained the smallest or tightest fold angle, about 5°, while Kapton of the same thickness retained a 125° angle. Papers generally outperformed polymers, with the exception of PETG. Among papers, origami paper retained a tighter fold angle than printer paper due to noticeably longer fibers increasing the stiffness and slightly lowering yield strain shown in Table 1. It was curious that PETG should maintain a tighter fold angle than even origami paper. To explain this, the nature of plastic deformation at the fold was investigated.

SEM micrographs of folded Kapton, PP, and PETG polymer films revealed localized damage as a result of stress concentration from folding. Both interior and exterior fold surfaces were examined in this study to observe similarities and differences between tension and compression behavior and are presented in Fig. 3. All polymer films showed wrinkling

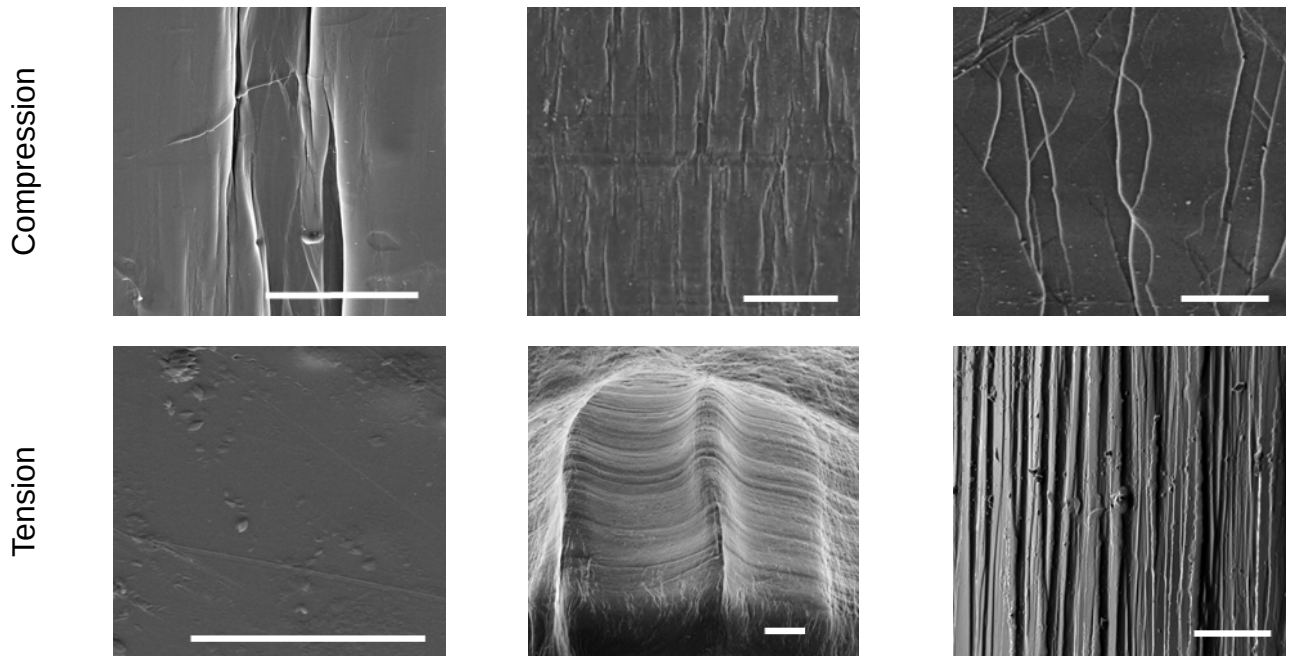

FIGURE 3: SEM MICROGRAPHS OF COMPRESSIVE AND TENSILE DEFORMATION RESULTING FROM FOLDING FOR KAPTON (a), PP (b), AND PETG (c). (SCALE BAR = 10 μm)

deformation on interior fold surfaces subjected to compressive stresses (Fig. 3(a), (b), (c)). Wrinkling in this manner shared some similarities with wrinkling of rubber blocks in bending [16, 17]. Adjusting R/t during fold formation with the parallel plate folding technique altered the size of wrinkling deformations. For example, an increased R/t from 2 to 3 in Kapton generated wrinkling deformations with smaller depths (163 to 73 nm). Kapton (Fig. 3(a)) appeared to undergo brittle deformation evidenced by crack-like features on the compressed interior surface. However, this did not yield high fold angle retention as might be expected due to lack of tensile deformation as discussed later. PP and PETG yielded in a more ductile manner with PETG producing larger wrinkling deformations as measured by a contact stylus profilometer correlating with improved fold angle retention. Height of wrinkling deformation on Kapton ranged from 200 to 250 nm independent of thickness when folded to R/t = 1. However, PETG possessed heights of 2,000 nm proving a strong material dependence on morphology of wrinkling deformations as a result of bending. Studies by others showed that paper deformed by both buckling and delamination due to compressive forces as a result of bending [15, 18]. However, unlike polymers, paper was not shown to suffer damage resulting from tensile stresses on the outer fold surface.

Examination of the exterior fold surfaces of polymer films by SEM, as shown in the second row of Fig. 3(a), (b), and (c), revealed PETG and PP were damaged as a result of tensile stresses. Interestingly, Kapton did not appear to sustain substantial tensile deformation as seen in Fig. 3(a). This was attributed to the brittle-type failure of Kapton in uniaxial tension tests which is typically characterized by abrupt failure with little to no plastic deformation. In contrast to Kapton, tensile yield occurred on the exterior fold surfaces of PP and PETG in the form of striations perpendicular to the direction of applied stress seen in Fig. 3(b) and (c). Striations on PETG were tightly packed, highly concentrated (1342 ± 867 striations/mm), well-aligned, and ranged in size from 0.2 – 2 μm. Similarly, PP striations were oriented perpendicular to the direction of tensile stress, but, within those striations, additional deformation (1137 ± 400 /mm) oriented parallel to the direction

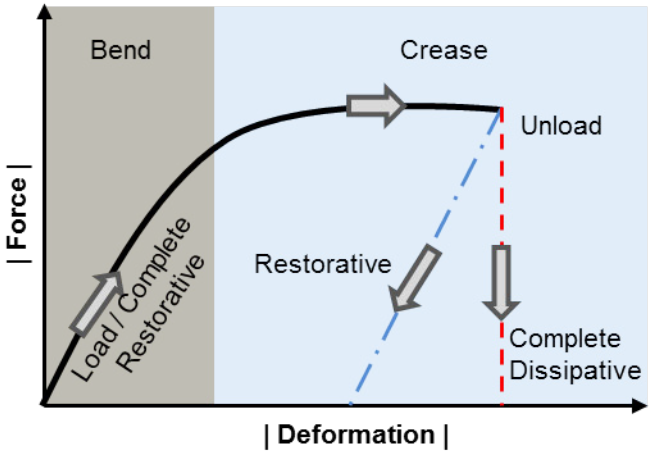

FIGURE 4: SCHEMATIC FORCE-DEFORMATION-RECOVERY BEHAVIOR OF POLYMERS

of tensile stress was observed. This was most likely caused by the matte surface finish of this particular PP specimen where the majority of the parallel striations were located within raised regions. Observing failure mechanisms visually explains relaxed fold angle results and informs the angle retention metric of fold performance.

The failure mechanisms observed by SEM and profilometry confirmed that fold retention is regulated by the type and intensity of plastic deformation and failure. The schematic force-deformation-recovery curve presented in Fig. 4 demonstrates three examples of behavior: complete restorative, restorative and complete dissipative. Complete restorative behavior involves complete energy recovery, for example an elastomer such as PDMS returns to its undeformed configuration after folding. Moderate restorative behavior (blue -·) is characterized by energy recovery to some degree leaving some residual deformation. Kapton exhibited moderate restorative behavior by wrinkling in compression, but not exhibiting permanent deformation in tension, resulting in large fold angles. PP also exhibited moderate restorative behavior, although it incurred more severe tensile and compressive deformations. Complete dissipative behavior (red --) involves no energy recovery upon unloading and no deformation is recovered. Delamination of paper is a type of nearly complete dissipative failure that results in favorable fold angle retention. PETG, which held the tightest residual fold angle, also exhibited nearly complete dissipative behavior, with permanent deformations displayed on both tension and compression surfaces. PETG also possessed the largest wrinkling deformations in terms of both width and height. Understanding the nature of plastic deformation and hence energy recoverability is the critical determining factor for fold angle retention and should be considered in material selection for origami applications.

CONCLUSIONS

An understanding of fold performance is critical for design of engineered origami structures and is ultimately material dependent. Fold angle retention, one of many metrics of fold performance, of polymer films was the primary focus here. Polymers can serve as substrates for active stimuli-responsive materials in actuating adaptive origami structures. Using a folding technique to overcome limitations of more conventional methods, it was found that failure behavior of polymer films is a key predictor of fold angle retention. Application-dependent fold angles can be achieved through material selection informed by knowledge of failure mechanisms.

Future work will involve developing a better understanding of how polymer microstructure (amorphous and semi-crystalline) and deformation mode (shear banding, crazing, cavitation, etc.) affect fold performance. Hypotheses developed from these experiments will then be tested on a larger material library noting any additional trends. Current and future work also includes identifying the bending strain at plastic deformation onset in real time. This measurement can be performed by directing a laser through a developing fold to detect the formation of surface deformations. It is anticipated that either well-aligned striations would result in beam scattering (akin to x-ray scattering), or stress whitening would serve as a beam stop, or both would occur. Strain at permanent deformation onset is a potential parameter for achievable fold angles of an undeformed state and is another factor that influences material selection.

ACKNOWLEDGMENTS

The authors would like to acknowledge the NSF and AFOSR for funding and Jared Needle for his origami expertise.

REFERENCES

[1] Zirbel, S.A., Lang, R.J., Thomson, M.W., Sigel, D.A., Walkemeyer, P.E., Trease, B.P., Magleby, S.P., Howell, L.L., 2013, "Accommodating Thickness in Origami-Based Deployable Arrays," *J. Mech. Design*, **135**(11), pp. 111005-1 – 111005-11.

[2] Fuchi, K., Tang, J., Crowgey, B., Diaz, A.R., Rotherll, E.J., Ouedraogo, R.O., 2012, "Origami Tunable Frequency Selective Surfaces," *IEEE Antennas Wireless Propag. Lett.*, **11,** pp. 473-475.

[3] Wu, W., and You, Z., 2013, "A Solution for Folding Rigid Tall Shopping Bags," *Proc. R. Soc. A*, **467**, pp. 2561-2574.

[4] Schenk, M., and Guest, S.D., 2011, "Origami Folding: A Structural Engineering Approach," *Origami 5: Fifth International Meeting of Origami Science, Mathematics, and Education*, P. Wang-Iverson et al., eds., CRC Press, Boca Raton, pp. 291-304.

[5] Tachi, T., 2010, "Geometric Considerations for the Design of Rigid Origami Structures," *Proceedings of IASS Symposium*, pp. 771-782.

[6] Liu, Y., Boyles, J.K., Genzer, J., Dickey, M., 2012, "Self-Folding of Polymer Sheets Using Local Light Absorption," *Soft Matter*, **8**(6), pp. 1764-1769.

[7] Kim, J,. Hanna, J., Hayward, R., Santangelo, D., 2012, "Thermally Responsive Rolling of Thin Gel Strips with Discrete Variations in Swelling," *Soft Matter*, **8**(8), pp. 2375-2381.

[8] Felton, S., Tolley, M., Shin, B., Onal, C., Demaine, E., Rus, D., Wood, R., 2013, "Self-Folding with Shape Memory Composites," *Soft Matter*, **9**(32), pp. 7688-7694.

[9] Ma, J., You, Z., 2013, "Energy Absorption of Thin-Walled Square Tubes With a Prefolded Origami Pattern – Part I: Geometry and Numerical Simulation," *J. Appl. Mech.*, **81**(1), pp. 011003-1 – 011003-11.

[10] Zhao, X., Hu, Y., Hagiwara, I., 2011, "Shape Optimization to Improve Energy Absorption Ability of Cylindrical Thin-Walled Origami Structure," *J. Comp. Sci. Technol.*, **5**(3), pp. 148-162.

[11] Beex, L.A.A., and Peerlings, R.H.J., 2009, "An Experimental and Computational Study of Laminated Paperboard Creasing and Folding," *Int. J. Solids Struc.*, **46**, pp. 4192-4207.

[12] Nagasawa, S., Fukuzawa, Y., Yamaguchi, T., Tsukatani, S., Katayama, I., 2003, “Effect of Crease Depth and Crease Deviation on Folding Deformation Characteristics of Coated Paperboard,” *J. Mater. Process. Tech.*, **140**, pp. 157-162.
[13] Nygards, M., Just, M., Tryding, J., 2009, “Experimental and Numerical Studies of Creasing of Paperboard,” *Int. J. Solids Struc.* **46**, pp. 2493-2505.
[14] Huang, H., Hagman, A., Nygards, N., 2014, “Quasi Static Analysis of Creasing and Folding for Three Paperboards,” *Mech. Mater.*, **69**(1), pp. 11-34.
[15] Carlsson, L., Fellers, C., De Ruvo, A., 1980, “The Mechanism of Failure in Bending of Paperboard,” *J. Mater. Sci.*, **15**, pp. 2636-2642.
[16] Gent, A.N., Cho, I.S., 1999, “Surface Instabilities in Compressed or Bent Rubber Blocks,” *Rubber Chem. Technol.*, **72**(2), pp. 253-262.
[17] Hohlfeld, E., Mahadevan, L., 2011, “Unfolding the Sulcus,” *Phys. Rev. Lett.*, **106**(10), pp. 105702.
[18] Yasuda, H., Yein, T., Tachi, T., Miura, K., Taya, M., 2013, “Folding Behavior of Tachi-Miura Polyhedron Bellows,” *Proc. R. Soc. A*, **469**(2159), pp. 20130351.